Weierstraß-Institut
für Angewandte Analysis und Stochastik

im Forschungsverbund Berlin e.V.

Preprint ISSN 0946 – 8633

Stochastic simulation method for a 2D elasticity problem with random loads

K. K. Sabelfeld[1,2], I. A. Shalimova[2], and A. I. Levykin[2]

[1] Weierstrass Institute for Applied Analysis and Stochastics, Mohrenstrase 39. D – 10117 Berlin, Germany; E-Mail: sabelfel@wias-berlin.de,

[2] Institute of Comp. Mathematics and Mathem. Geophysics, Russian Acad. Sci., Lavrentiev, 6, 630090 Novosibirsk, Russia

No. 1217

Berlin 2007

1991 *Mathematics Subject Classification.* 65C05, 65C20, 65Z05.

Key words and phrases. Isotropic Random Fields, Spectral Tensor, Poisson integral formula, Random Walk on Fixed Spheres, Lamé equation, Successive Over Relaxation Method, Transverse and Longitudinal Correlations.

This work is supported partly by the program of Leading Scientific Schools under Grant N 4774.2006.1, the RFBR Grant N 06-01-00498, DFG Grants 436 RUS 17/24/05, Sa 861/4-1, and NATO Collaborative Linkage Grant CLG N 981426.

Edited by
Weierstraß-Institut für Angewandte Analysis und Stochastik (WIAS)
Mohrenstraße 39
10117 Berlin
Germany

Fax: + 49 30 2044975
E-Mail: preprint@wias-berlin.de
World Wide Web: http://www.wias-berlin.de/

Abstract

We develop a stochastic simulation method for a numerical solution of the Lamé equation with random loads. To treat the general case of large intensity of random loads, we use the Random Walk on Fixed Spheres (RWFS) method described in our paper [20]. The vector random field of loads which stands in the right-hand-side of the system of elasticity equations is simulated by the Randomization Spectral method presented in [16] and recently revised and generalized in [8]. Comparative analysis of RWFS method and an alternative direct evaluation of the correlation tensor of the solution is made. We derive also a closed boundary value problem for the correlation tensor of the solution which is applicable in the case of inhomogeneous random loads. Calculations of the longitudinal and transverse correlations are presented for a domain which is a union of two arbitrarily overlapped discs. We also discuss a possibility to solve an inverse problem of determination of the elastic constants from the known longitudinal and transverse correlations of the loads.

1. Introduction

It is well known that the boundary value problems with random parameters are very interesting models which become more and more popular in many fields of science and technology, especially in problems where the data are highly irregular, for instance, like in the case of turbulent transport [10], flows in porous medium [2], or evaluation of elastic properties of polymers and composites containing fibers which are randomly oriented in a plane [11], [7], and in elastography imaging [13]. In [9], a stochastic model that could realistically and accurately simulate wind loads that are generated by thunderstorm downbursts for transmission line design is developed.

In conventional deterministic numerical methods, these problems are solved as follows: first one constructs a synthesized sample of the input random parameter; then the obtained deterministic equation is solved numerically, say, by finite element method and give the solution in all points of the grid domain. These two steps are repeated many times, so that the obtained statistics is enough to calculate the desired averages accurate enough. In [1], [11], [14], [22], this approach is used in stochastic finite element methods. Obviously, this technique is generally time consuming, and to solve practically interesting problems one needs supercomputers to extract sufficient statistical information.

In the Monte Carlo approach, the algorithms are designed so that the solution is calculated only in the desired set of points without constructing the solution in the whole domain [4], [15], [17], [16]. To evaluate different statistical characteristics of random boundary value problems we use the Double Randomization technique (e.g., see [16]). This approach is possible if the desired statistical characteristics

(e.g., the mean or the correlation tensor) can be represented in the form of a double expectation over the input random parameters, and over the trajectories of a Markov process used in a stochastic estimator for solving the deterministic equation. The advantage of this method is that we have no need to solve the equation many times, hence, the cost of this method is drastically decreased compared to the stochastic finite element method.

The approach we use in the present paper is based on the Poisson type integral formula written for each disc of a domain consisting of a family of overlapping discs. We call this method a Random Walk on Fixed Spheres algorithm (RWFS). The original differential boundary value problem is equivalently reformulated in the form of a system of integral equations defined on the intersection surfaces (arches, in 2D, and caps, if generalized to 3D spheres). To solve the obtained system of integral equations, a Random Walk procedure is constructed where the random walks are living on the intersection surfaces. Since the discs (spheres) are fixed, it is convenient to construct also discrete random walk methods for solving the system of linear equations approximating the system of integral equations.

In [20] we have concluded that in the case of classical potential theory, the Random Walk on Fixed Spheres considerably improves the convergence rate of the standard Random Walk on Spheres method. More interesting, we succeeded there to extend the algorithm to the system of Lamé equations which cannot be solved by the conventional Random Walk on Spheres method. Therefore, we are able to use this method in our numerical analysis of the Lamé equation with random loads. The 2D vector random load is assumed to be incompressible, isotropic and Gaussian, with a given form of the spectral tensor which in the studied case is uniquely defined by one scalar function, the energy spectrum. To simulate this vector random field we apply the Randomization Spectral Method presented in details in our recent paper [8].

The paper is organized as follows. In section 2, we present shortly the Random Walk on Fixed Spheres algorithm: in section 2.1 we give the integral formulation of the Lamé equation, and in section 2.2 we describe a discrete approximation of the given integral equations and mention two stochastic methods based on Random Walk algorithms for solving linear systems. This material can be found in more details in our previous paper [20].

In this paper we deal with random loads, so a generalization of Random Walk on Fixed Spheres algorithm to the Lamé equation with non-zero body forces is needed which is done in section 2.3. Here we present in details a Direct and Adjoint stochastic algorithms.

In section 3 we describe the random loads, and the Randomization Spectral method for simulation these vector random fields. Section 4 deals with an alternative method of calculation of the correlation tensor of the solution of Lamé equation based on its closed representation in the form of an iterated integral Green formula. The relevant boundary value problem for the correlation tensor is also derived.

Numerical results are presented in section 5. In section 5.1 we test the random field simulation method by comparing calculations with exact results. The Random Walk on Fixed Spheres method for the case of non-zero body forces is tested in section 5.2 by solving a test problem with known exact solution. The main numerical results are presented in section 5.3 where we give the results of numerical calculations of the longitudinal and transverse correlations of the displacement vector under random loads.

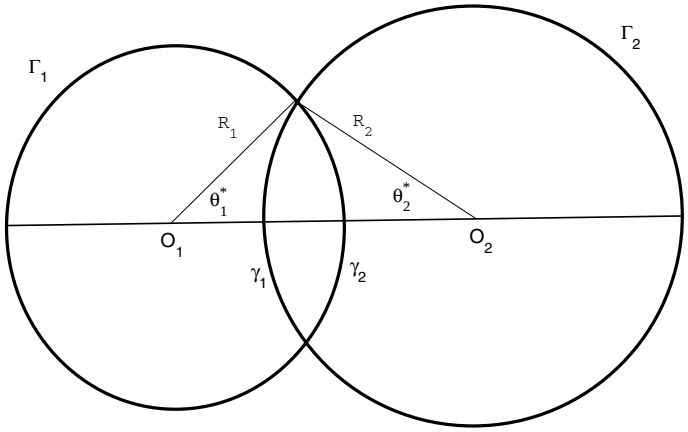

Figure 1: Two overlapping discs illustrating the main notations.

2. The system of Lamé equations

In this section we extend the Random Walk on Fixed Spheres (RWFS) algorithm described in our previous paper [20] to the Lamé equation with non-zero body forces. To make the presentation closed, we first describe shortly the method for the case of zero body forces.

2.1 Homogeneous case: zero body forces

In [20], we developed a Random Walk on Fixed Spheres algorithm for a special class of 2D domains consisting of a set of overlapped discs. The main idea of the method can be explained for the simplest case, when the domain consists of two overlapping discs.

Let us consider a finite two-dimensional elastic body D which consists of two overlapping discs $K(\mathbf{x}_0^{(1)}, R_1)$ and $K(\mathbf{x}_0^{(2)}, R_2)$ centered at $O_1 = \mathbf{x}_0^{(1)}$ and $O_2 = \mathbf{x}_0^{(2)}$ (see Figure 1):

$$D = K(\mathbf{x}_0^{(1)}, R_1) \cup K(\mathbf{x}_0^{(2)}, R_2); \quad K(\mathbf{x}_0^{(1)}, R_1) \cap K(\mathbf{x}_0^{(2)}, R_2) \neq \emptyset \,. \tag{2.1}$$

We denote by γ_2 the part of the circle $S(\mathbf{x}_0^{(1)}, R_1) = \partial K(\mathbf{x}_0^{(1)}, R_1)$ which belongs to the second disc while Γ_1 is the part of the circle $S(\mathbf{x}_0^{(1)}, R_1)$ not belonging to the second disc; analogously γ_1 and Γ_2 are defined. So the boundary of the domain D consists of Γ_1 and Γ_2, and $\gamma = \gamma_1 \cup \gamma_2$ is the phase space of the integral equation to be constructed. We also introduce angles θ_1^* and θ_2^* so that $2\theta_1^*$ is the angle of view of the arc γ_2 from the centre of the first circle, and $2\theta_2^*$ is the angle of view of the arc γ_1 from the centre of the second circle as shown in Figure 1.

Let D be a homogeneous isotropic elastic body with a boundary $\Gamma = \partial D$ whose state in the absence of

body forces is governed by the classical static elasticity equation, the Lamé equation, (e.g., see [18]):

$$\Delta \mathbf{u}(\mathbf{x}) + \alpha \operatorname{grad} \operatorname{div} \mathbf{u}(\mathbf{x}) = 0, \quad \mathbf{x} \in D, \tag{2.2}$$

where $\mathbf{u}(\mathbf{x}) = (u_1(x_1,x_2), u_2(x_1,x_2))$ is a vector of displacements, whose components are real-valued regular functions. The elastic constant α

$$\alpha = \frac{\lambda + \mu}{\mu}$$

is expressed through the Lamé constants of elasticity λ and μ. It can be expressed through the Poisson ratio $\nu = \lambda/2(\lambda+\mu)$ as follows: $\alpha = 1/(1-2\nu)$. The Poisson ratio characterizes the relative amount of the change of the transverse to longitudinal displacements. It is known that due to thermodynamical reasons ν is bounded between $-1 \le \nu < 0.5$. This implies for α: $1/3 \le \alpha < \infty$. So there are materials with negative values of ν (α varies in $1/3 \le \alpha \le 1$), and materials with $\nu \approx 0.5$. The last case is very difficult for conventional numerical methods.

The first boundary value problem for the Lamé equation consists in finding a vector function $\mathbf{u} \in C^2(D) \cap C(\bar{D})$ satisfying the boundary condition

$$\mathbf{u}(\mathbf{y}) = \mathbf{g}(\mathbf{y}), \quad \mathbf{y} \in \Gamma \tag{2.3}$$

where $\mathbf{g} \in C(\Gamma)$ is a given vector-function.

Let us consider an arbitrary point $\mathbf{x} = (x_1, x_2)$ with polar coordinates (r, φ') inside a disc $K(\mathbf{x}_0, R)$ centered at $\mathbf{x}_0 = (x_{01}, x_{02})$. The point $\mathbf{y} = (y_1, y_2)$ situated on the circle $S(\mathbf{x}_0, R)$ has the coordinates (R, θ), where $\theta = \varphi' + \beta$, and z is defined by $\mathbf{z} = \mathbf{y} - \mathbf{x}$, β is the angle between the vectors $\mathbf{x}$ and $\mathbf{y}$; ψ is the angle between $\mathbf{x}$ and $\mathbf{z}$. Define also the angle φ by $\varphi = \varphi' + \psi$. The following statement given in [18] is a generalization of the Poisson formula:

Theorem 2.1. *The solution to the equation (2.2) satisfies the following spherical mean value relation,* $\mathbf{x}$ *being an arbitrary point in* $K(\mathbf{x}_0, R)$*:*

$$u_i(\mathbf{x}) = \frac{R^2 - |\mathbf{x} - \mathbf{x}_0|^2}{2\pi R} \sum_{j=1}^{2} \int_{S(\mathbf{x}_0,R)} \frac{b_{ij}(\mathbf{x},\mathbf{y})\, u_j(\mathbf{y})}{|\mathbf{x}-\mathbf{y}|^2}\, dS_{\mathbf{y}}\,, \quad i = 1,2, \tag{2.4}$$

where b_{ij} *are functions of* $\mathbf{x}, \mathbf{y}$*, explicitly represented as the entries of the following matrix*

$$B(\mathbf{x},\mathbf{y}) = \frac{\alpha}{\alpha+2} \begin{pmatrix} \frac{2}{\alpha} + 2\cos^2\varphi + \frac{|\mathbf{x}-\mathbf{y}|}{R}\cos(\theta+\varphi) & 2\cos\varphi\sin\varphi + \frac{|\mathbf{x}-\mathbf{y}|}{R}\sin(\theta+\varphi) \\ 2\cos\varphi\sin\varphi + \frac{|\mathbf{x}-\mathbf{y}|}{R}\sin(\theta+\varphi) & \frac{2}{\alpha} + 2\sin^2\varphi - \frac{|\mathbf{x}-\mathbf{y}|}{R}\cos(\theta+\varphi)\,. \end{pmatrix}$$

Since by definition we have

$$\cos\theta = \frac{y_1 - x_{01}}{R}, \quad \sin\theta = \frac{y_2 - x_{02}}{R}, \quad \cos\varphi = \frac{y_1 - x_1}{|\mathbf{x}-\mathbf{y}|}, \quad \sin\varphi = \frac{y_2 - x_2}{|\mathbf{x}-\mathbf{y}|},$$

we get for $b_{ij} = b_{ij}(\mathbf{x},\mathbf{y})$, $i,j = 1,2$:

$$b_{11} = 1 + \frac{\alpha}{\alpha+2}\left[\frac{(y_1-x_1)^2-(y_2-x_2)^2}{|\mathbf{x}-\mathbf{y}|^2} + \frac{(y_1-x_1)(y_1-x_{01})-(y_2-x_2)(y_2-x_{02})}{R^2}\right],$$

$$b_{22} = 1 - \frac{\alpha}{\alpha+2}\left[\frac{(y_1-x_1)^2-(y_2-x_2)^2}{|\mathbf{x}-\mathbf{y}|^2} - \frac{(y_1-x_1)(y_1-x_{01})-(y_2-x_2)(y_2-x_{02})}{R^2}\right],$$

$$b_{12} = b_{21} = \frac{\alpha}{\alpha+2}\left[2\frac{(y_1-x_1)(y_2-x_2)}{|\mathbf{x}-\mathbf{y}|^2} + \frac{(y_2-x_2)(y_1-x_{01})+(y_1-x_1)(y_2-x_{02})}{R^2}\right].$$

Let us define a function for points $\mathbf{x}$ in the first disc $K(\mathbf{x}_0^{(1)}, R_1)$

$$p_{R_1}(\mathbf{y};\mathbf{x}) = \frac{R_1^2 - |\mathbf{x}-\mathbf{x}_0^{(1)}|^2}{2\pi R_1} \cdot \frac{1}{|\mathbf{x}-\mathbf{y}|^2}\ . \tag{2.5}$$

We note that $p_{R_1}(\mathbf{x},\mathbf{y})$ is a probability density function of the variable $\mathbf{y} \in S(\mathbf{x}_0^{(1)}, R_1)$, for all $\mathbf{x} \in K(\mathbf{x}_0^{(1)}, R_1)$; sampling algorithm from this density is described in [6] and in a bit different form in [19]. Analogously, $p_{R_2}(\mathbf{y};\mathbf{x})$ is defined for points $\mathbf{x}$ in the second disc $K(\mathbf{x}_0^{(2)}, R_2)$.

In the notation of $p_{R_1}(\mathbf{y};\mathbf{x})$, the relation (2.4) written for the points $\mathbf{x}$ in the first disc reads in the matrix form:

$$\mathbf{u}(\mathbf{x}) = \int\limits_{S(\mathbf{x}_0^{(1)},R_1)} p_{R_1}(\mathbf{y};\mathbf{x})\, B(\mathbf{x},\mathbf{y})\, \mathbf{u}(\mathbf{y})\, dS(\mathbf{y})\ . \tag{2.6}$$

Taking analogous representation for points of the second disc, we arrive at a system of 4 integral equations defined on the arches γ_1 and γ_2. Indeed, using the notations $v_1^{(1)}(\mathbf{x}) = u_1(\mathbf{x})$ and $v_1^{(2)}(\mathbf{x}) = u_2(\mathbf{x})$ for $\mathbf{x} \in \gamma_1$, and $v_2^{(1)}(\mathbf{x}) = u_1(\mathbf{x})$ and $v_2^{(2)}(\mathbf{x}) = u_2(\mathbf{x})$ for $\mathbf{x} \in \gamma_2$ we get

$$\mathbf{v} = G\mathbf{v} + \mathbf{F}, \tag{2.7}$$

or, in more details,

$$\begin{pmatrix} v_1^{(1)} \\ v_1^{(2)} \\ v_2^{(1)} \\ v_2^{(2)} \end{pmatrix} = \begin{pmatrix} 0 & 0 & B_{11} & B_{12} \\ 0 & 0 & B_{21} & B_{22} \\ \hat{B}_{11} & \hat{B}_{12} & 0 & 0 \\ \hat{B}_{21} & \hat{B}_{22} & 0 & 0 \end{pmatrix} \begin{pmatrix} v_1^{(1)} \\ v_1^{(2)} \\ v_2^{(1)} \\ v_2^{(2)} \end{pmatrix} + \begin{pmatrix} f_1^{(1)} \\ f_1^{(2)} \\ f_2^{(1)} \\ f_2^{(2)} \end{pmatrix} \tag{2.8}$$

where the integral operators B_{ij}, $i,j = 1,2$ are defined, according to (2.4), for the points of the first disc $\mathbf{x} \in K(\mathbf{x}_0^{(1)}, R_1)$:

$$B_{ij}\, v_2^{(j)}(\mathbf{x}) = \int\limits_{\gamma_2} p_{R_1}(\mathbf{y};\mathbf{x})\, b_{ij}(\mathbf{x},\mathbf{y})\, v_2^{(j)}(\mathbf{y})\, dS(\mathbf{y}), \quad i,j = 1,2\ ,$$

while the integral operators $\hat{B}_{ij}$, $i,j = 1,2$ are defined for the points of the second disc $\mathbf{x} \in K(\mathbf{x}_0^{(2)}, R_2)$:

$$\hat{B}_{ij}\, v_1^{(j)}(\mathbf{x}) = \int\limits_{\gamma_1} p_{R_2}(\mathbf{y};\mathbf{x})\, b_{ij}(\mathbf{x},\mathbf{y})\, v_1^{(j)}(\mathbf{y})\, dS(\mathbf{y}), \quad i,j = 1,2\ .$$

The functions f_i^j are defined analogously:

$$f_i^{(j)}(\mathbf{x}) = \sum_{k=1}^{2} \int_{\Gamma_i} p_{R_i}(\mathbf{y};\mathbf{x})\, b_{jk}(\mathbf{x},\mathbf{y})\, g_k(\mathbf{y})\, dS(\mathbf{y}), \quad i,j = 1,2\ .$$

It should be noted that the equivalence of the system (2.8) and the boundary value problem (2.2), (2.3) is not evident, in contrast to the case of the Laplace equation. Indeed, the L_1-norm of the integral operator G is generally larger than 1, so we have to use finer properties. Indeed, let us estimate the L_1-norm. In [20] we derived the following estimation

$$\|G\|_{L_1} \le \frac{2+4\sqrt{2}\alpha}{\alpha+2}\left(1-\frac{\theta_1^*}{\pi}-\frac{\theta_2^*}{\pi}\right) \tag{2.9}$$

where θ_1^* and θ_2^* are the view angles defined above.

This estimation shows that $\|G\|_{L_1}$ can be made less than 1 for a fixed value of α by a proper choice of θ_1^*, θ_2^* which would imply a restriction of the overlapping configuration. To be free of such a restriction, the spectral radius should be estimated. In [20] we have used the result obtained by S.L. Sobolev [21] to prove the following statement.

Theorem 2.2. *The integral operator G of the system (2.8) is a Fredholm operator with kernels continuous on $\mathbf{x} \in \gamma_1$ and $\mathbf{y} \in \gamma_2$, with the same type of singularities at the points of intersections of the arches γ_1 and γ_2 as the singularities in the case of Laplace equation ($\alpha = 0$): $p(\mathbf{y};\mathbf{x}) \simeq \frac{\sin(\theta_1^*+\theta_2^*)}{\pi|\mathbf{x}-\mathbf{y}|}$ as $\mathbf{x} \to \mathbf{y}$. The spectral radius of G is less than 1 for any nonempty overlapping, which ensures the equivalence of the system (2.8) and the boundary value problem (2.2), (2.3).*

This result implies that: (1), instead of the original boundary value problem, we can solve the equivalent integral equation (2.8), and (2), the Fredholm integral equation (2.8) can be approximated by a system of linear algebraic equations.

2.2 Approximation by a system of linear algebraic equations

Let us approximate the system of integral equations (2.8) by a system of linear algebraic equations. We choose a set of nodes $\mathbf{x}_1,\dots,\mathbf{x}_{m_1+1}$ uniformly on the arc γ_1 and $\mathbf{y}_1,\dots,\mathbf{y}_{m_2+1}$ on γ_2 generating by the uniform polar angles distributions (the end points are included). These meshes subdivide γ_1 and γ_2 in the set of arches $\gamma_1^{(i)}$, $i = 1,\dots,m_1$ and $\gamma_2^{(i)}, i = 1,\dots,m_2$, respectively. Of course, the nodes can be chosen not uniformly, say, according to some distribution which generates the nodes more densely around the singular points where the arches do intersect.

Since the Poisson kernel $p(\mathbf{y};\mathbf{x})$ has a singularity, it is convenient to take the approximation in the form:

$$\int_{\gamma_1} p_{R_2}(\mathbf{x};\mathbf{y}_k)\, b_{ij}(\mathbf{y}_k,\mathbf{x})\, v_2^{(j)}(\mathbf{x}) dS_{\mathbf{x}} = \sum_{i=1}^{m_1+1} p_i^{(1)}(\mathbf{x}_i,\mathbf{y}_k)\, b_{ij}(\mathbf{y}_k,\mathbf{x}_i)\, v_2(\mathbf{x}_i), \quad k = 2,\dots,m_2,$$

and analogously,

$$\int_{\gamma_2} p_{R_1}(\mathbf{x}';\mathbf{x}_k) b_{ij}(\mathbf{x}_k,\mathbf{x}') v_1^{(j)}(\mathbf{x}') dS_{\mathbf{x}'} = \sum_{i=1}^{m_2+1} p_i^{(2)}(\mathbf{y}_i,\mathbf{x}_k) b_{ij}(\mathbf{x}_k,\mathbf{y}_i)\, v_1(\mathbf{y}_i), \quad k = 2,\dots,m_1,$$

where

$$p_i^{(1)}(\mathbf{x}_i,\mathbf{y}_k)=\int\limits_{\gamma_1^{(i)}} p_{R_2}(\mathbf{y};\mathbf{y}_k)dS_{\mathbf{y}}\ ,\quad p_i^{(2)}(\mathbf{y}_i,\mathbf{x}_k)=\int\limits_{\gamma_2^{(i)}} p_{R_1}(\mathbf{x}';\mathbf{x}_k)dS_{\mathbf{x}'}\ . \tag{2.10}$$

These coefficients can be evaluated explicitly, see [20]. The same approximation is used to calculate the right-hand side vector in (2.8) $\mathbf{F}=(f_1^{(1)},f_1^{(2)},f_2^{(1)},f_2^{(2)})^T$ in all grid points on $\Gamma=\Gamma_1\cup\Gamma_2$.

Thus we come to a discrete approximation of the system of integral equations (2.8) in the form of the following system of linear algebraic equations:

$$w^{(k)}=\sum_{i=1}^{m_1+m_2} a_{ik}\,w^{(k)}+F^{(k)},\quad k=1,\ldots,m_1+m_2\ , \tag{2.11}$$

or in a matrix form $\mathbf{w}=A\mathbf{w}+\hat{\mathbf{F}}$.

Here the column-vector $\mathbf{w}=(\mathbf{w}_1^{(1)},\mathbf{w}_1^{(2)},\mathbf{w}_2^{(1)},\mathbf{w}_2^{(2)})^T$ consists of four column-vectors which are the relevant approximations of the solution $\mathbf{v}=(v_1^{(1)},v_1^{(2)},v_2^{(1)},v_2^{(2)})^T$. The same for the vector-function $\mathbf{F}$ and vector $\hat{\mathbf{F}}$.

Note that the matrix A is a square 2×2-block-matrix, it consists of zero diagonal blocks, and rectangular blocks A_{12} and A_{21} relating the vectors $(\mathbf{w}_1^{(1)},\mathbf{w}_1^{(2)})^T$ and $(\mathbf{w}_2^{(1)},\mathbf{w}_2^{(2)})^T$.

The linear system (2.11) can be solved numerically, by an iteration method, or even by a direct inversion if the number of nodes on the arches is not too large. In [20], for a class of so-called DS_2-domains we developed an iteration procedure based on the SOR method, which converges much faster than the standard simple iterations. Based on this procedure, we constructed a Random Walk algorithm for solving (2.11) which converges very fast.

Let us shortly describe the SOR procedure. Let L and U be the left- and right triangular matrices of the matrix A. Since the diagonal blocks of A are zero blocks, we have $A=L+U$. Let ω be an arbitrary parameter of the SOR method, then by simple transformations we arrive at the following equivalent form of the equation (2.11):

$$\mathbf{w}=T_\omega\mathbf{w}+\mathbf{d}$$

where

$$T_\omega=(I-\omega L)^{-1}\big[(1-\omega)I+\omega U\big]\mathbf{w},$$

and $\mathbf{d}=\omega(I-\omega L)^{-1}\hat{\mathbf{F}}$. We use here the notation I for the identity matrix.

Since however for the DS_2-domains (our two overlapping discs belong to this class) we have the following remarkable property: $(I-\omega L)^{-1}=(I+\omega L)$, the new transition matrix is given explicitly by

$$T_\omega=(I+\omega L)\big[(1-\omega)I+\omega U\big]\ ,$$

and the right-hand side $\mathbf{d}=\omega(I+\omega L)\hat{\mathbf{F}}$.

There are explicitly given relations between the eigenvalues of matrices A and T_ω, see [12], [20]. As to the convergence of the Random Walk algorithms, we illustrate it by the comparison of spectral radii for the matrices A and $T=T_{\omega=1}$. Note that to have finite variance, these algorithms require also that $\rho(A^2/p)<1$ for the standard Random Walk method, and $\rho(T^2/p)<1$ for the SOR based Random Walk

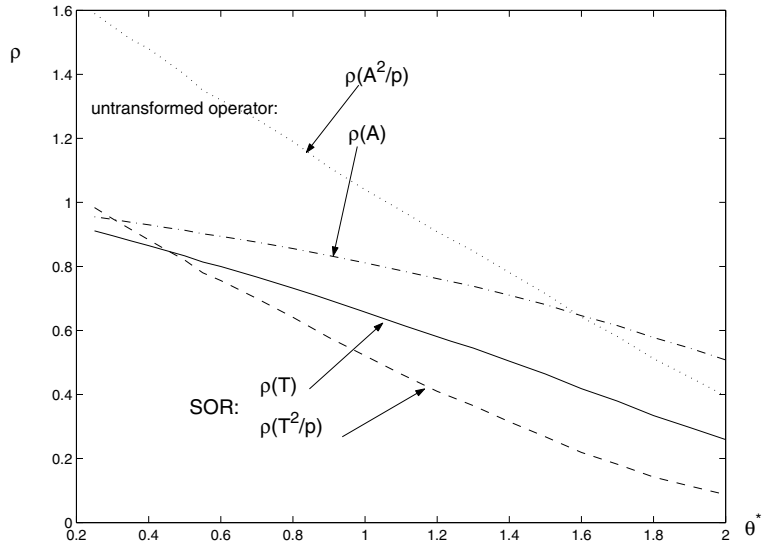

Figure 2: The spectral radii of the SOR operator T, and T^2/p, and for the simple iteration operator A and A^2/p, as functions of θ^*, for two overlapping discs of unit radii. The Lamé equation with $\alpha = 2.5$.

algorithm. In Figure 2 we show all these spectral radii as functions of $\theta^* = \theta_1^* + \theta_2^*$ which characterizes the amount of overlapping of our two discs. It is seen that the standard Random Walk method can be applied only for relative large overlappings while the SOR based Random Walk algorithm converges for arbitrary overlappings, and moreover, the convergence is much faster.

Finally we note that our system of linear equations gives the solution only for the points on the arches γ_1 and γ_2. For any other points, the solutions is obtained from the spherical mean representation formula (2.4) in the relevant disc.

2.3 Lamé equation with non-zero body forces

Now we extend the method to the case when there are body forces. The state of the body with fixed boundary is then governed by the following inhomogeneous Lamé equation

$$\Delta \mathbf{u}(\mathbf{x}) + \alpha \operatorname{grad} \operatorname{div} \mathbf{u}(\mathbf{x}) + \mathbf{f}(\mathbf{x}) = 0, \quad \mathbf{x} \in D, \quad \mathbf{u}|_\Gamma = 0. \tag{2.12}$$

Here $\mathbf{f}(\mathbf{x}) = \mathbf{g}(\mathbf{x})/\mu$ where $\mathbf{g}(\mathbf{x})$ describes the body forces.

The solution to the problem (2.12) can be represented through the solution of the problem (2.2). Indeed,

$$\mathbf{u}(\mathbf{x}) = \int_D G(\mathbf{x},\mathbf{y})\mathbf{f}(\mathbf{y})\, d\mathbf{y} \ . \tag{2.13}$$

We take the Green tensor $G(\mathbf{x},\mathbf{y})$ in the form

$$G(\mathbf{x},\mathbf{y}) = \Gamma(\mathbf{x}-\mathbf{y}) + W(\mathbf{x},\mathbf{y}) \tag{2.14}$$

where the tensor $\Gamma(\mathbf{x}-\mathbf{y})$ is the fundamental solution of the Lamé equation which in 2D case is given by [3]

$$\Gamma(\mathbf{x}-\mathbf{y}) = \frac{1}{8\pi}\left[(\bar{\alpha}\log|\mathbf{x}-\mathbf{y}|)\,\mathsf{I} - \frac{\bar{\beta}}{|\mathbf{x}-\mathbf{y}|^2}\,Q_{\mathbf{xy}}\right]. \tag{2.15}$$

Here $Q_{\mathbf{xy}}$ is a $2D$-matrix with the entries $Q_{ij} = (x_i - y_i)(x_j - y_j)$, $i, j = 1,2$, I is an identity matrix, and the constants $\bar{\alpha}$, $\bar{\beta}$ are expressed through the constant α as follows:

$$\bar{\alpha} = \frac{1+\alpha}{0.5+\alpha}, \quad \bar{\beta} = \frac{\alpha}{0.5+\alpha}\,.$$

Let us introduce some notations. Let $L = \Delta + \alpha\,\mathrm{grad}\,\mathrm{div}$ be the Lamé operator which is defined in (2.12) as a differential operator acting on a column-vector function $\mathbf{u}(\mathbf{x})$. If $W(\mathbf{x})$ is a 2×2-matrix with the first column $\mathbf{W}^{(1)}$ and second column $\mathbf{W}^{(2)}$, then we define $LW(\mathbf{x})$ as a matrix whose first column is $L\mathbf{W}^{(1)}(\mathbf{x})$, and the second column is $L\mathbf{W}^{(2)}(\mathbf{x})$. Analogously we define an "adjoint" operator $\hat{L}$ which acts on the rows of W, which actually implies that $\hat{L}W(\mathbf{x}) = LW^T(\mathbf{x})$.

Let us now consider the column-vectors consisting of the relevant entries of the matrices Γ and W in (2.14): $\Gamma^{(i)} = (\Gamma_{i1}, \Gamma_{i2})^T$, and $\mathbf{W}^{(i)} = (W_{i1}, W_{i2})^T$, $i = 1,2$.

From (2.14) it follows that the vector functions $\mathbf{W}^{(i)}(\mathbf{x},\mathbf{y})$, $i = 1,2$ solve the following pair of boundary value problems:

$$\Delta\mathbf{W}^{(i)}(\mathbf{x},\mathbf{y}) + \alpha\,\mathrm{grad}\,\mathrm{div}\,\mathbf{W}^{(i)}(\mathbf{x},\mathbf{y}) = 0, \quad \mathbf{x}\in D, \quad \mathbf{W}^{(i)}(\mathbf{x},\mathbf{y})|_{\mathbf{x}\to\mathbf{z}\in\partial D} = -\Gamma^{(i)}(\mathbf{z}-\mathbf{y}), \quad i = 1,2\,. \tag{2.16}$$

The integral representation (2.13) can be very conveniently used for the Monte Carlo calculations. Let us describe the method which we call a Double Randomization technique (for details, see [16]).

First, we rewrite the integral (2.13) in the form of an expectation. To this end, we introduce in the domain D an arbitrary probability density function $\pi(\mathbf{y})$ satisfying the condition that $\pi(\mathbf{y}) \neq 0$ for all points $\mathbf{y}\in D$ where $G(\mathbf{x},\mathbf{y})\mathbf{f}(\mathbf{y}) \neq 0$.

In particular, we could choose a uniform density so that the samples $\tilde{\mathbf{y}}$ from $\pi(\mathbf{y})$ are uniformly distributed in D.

Let us denote by E_π the expectation taken according to the distribution density $\pi(\mathbf{y})$. Then (2.13) can be written as follows

$$\mathbf{u}(\mathbf{x}) = \int_D \frac{G(\mathbf{x},\mathbf{y})\mathbf{f}(\mathbf{y})}{\pi(\mathbf{y})}\,\pi(\mathbf{y})d\mathbf{y} \;= E_\pi\left[\frac{G(\mathbf{x},\tilde{\mathbf{y}})\mathbf{f}(\tilde{\mathbf{y}})}{\pi(\tilde{\mathbf{y}})}\right] \tag{2.17}$$

where the points $\tilde{\mathbf{y}}$ are sampled in D from the density $\pi(\mathbf{y})$. In view of (2.14) we get

$$\mathbf{u}(\mathbf{x}) = E_\pi\left[\left\{\Gamma(\mathbf{x}-\tilde{\mathbf{y}}) + W(\mathbf{x},\tilde{\mathbf{y}})\right\}\frac{\mathbf{f}(\tilde{\mathbf{y}})}{\pi(\tilde{\mathbf{y}})}\right] \tag{2.18}$$

where the entries of the matrix $W(\mathbf{x},\mathbf{y})$ solve the boundary value problem (2.16). This problem is solved by our Random Walk Method which conveniently finds the solutions on the arches γ_1 and γ_2 without calculating the solution in the whole domain. We can use this feature to construct very efficient method based on the representation (2.18) rewritten as follows. Indeed, using the spherical mean representation

(2.4) for the vector functions $\mathbf{W}^{(i)}$ defined in (2.16) and assuming they are already found on the arches γ_1 and γ_2 we arrive at the following probabilistic representation

$$\mathbf{u}(\mathbf{x}) = E_\pi \left[\left\{ \Gamma(\mathbf{x}-\tilde{\mathbf{y}}) - \langle\, B(\mathbf{x},\tilde{\mathbf{z}})\,\Gamma(\tilde{\mathbf{z}}-\tilde{\mathbf{y}}) \,|\, \tilde{\mathbf{y}} \,\rangle_{\tilde{\mathbf{z}}\in\Gamma_i} + \langle\, B(\mathbf{x},\tilde{\mathbf{z}})\,W(\tilde{\mathbf{z}},\tilde{\mathbf{y}}) \,|\, \tilde{\mathbf{y}} \,\rangle_{\tilde{\mathbf{z}}\in\gamma_j} \right\} \frac{\mathbf{f}(\tilde{\mathbf{y}})}{\pi(\tilde{\mathbf{y}})} \right] . \tag{2.19}$$

Here the conditional expectation $\langle B(\mathbf{x},\tilde{\mathbf{z}})\,\Gamma(\tilde{\mathbf{z}}-\tilde{\mathbf{y}}) \,|\, \tilde{\mathbf{y}} \rangle_{\tilde{\mathbf{z}}}$ is taken according to a distribution of random points $\tilde{\mathbf{z}}$ on the relevant circle, the distribution density being $p(\mathbf{z};\mathbf{x})$ under the condition that the random point $\tilde{\mathbf{y}}$ (sampled in D from $\pi(\mathbf{y})$) is fixed: so if $\tilde{\mathbf{y}} \in K(O_i,R_i)$, then the sampled random point $\tilde{\mathbf{z}}$ lies on the circle $S(O_i,R_i)$, $i = 1,2$.

Let us rewrite (2.19) in a form more convenient for practical calculations:

$$\mathbf{u}(\mathbf{x}) = E_\pi \left[\left\{ \Gamma(\mathbf{x}-\tilde{\mathbf{y}}) + \langle\, B(\mathbf{x},\tilde{\mathbf{z}})\,V(\tilde{\mathbf{z}},\tilde{\mathbf{y}}) \,|\, \tilde{\mathbf{y}} \,\rangle_{\tilde{\mathbf{z}}\in S(O_i,R_i)} \right\} \frac{\mathbf{f}(\tilde{\mathbf{y}})}{\pi(\tilde{\mathbf{y}})} \right] \tag{2.20}$$

where the matrix $V(\mathbf{x},\tilde{\mathbf{z}})$ equals to $-\Gamma(\tilde{\mathbf{z}}-\tilde{\mathbf{y}})$ if the sampled point $\tilde{\mathbf{z}}$ lies on the external boundaries Γ_1 or Γ_2; if $\tilde{\mathbf{z}} \in \gamma$, then the matrix $V(\mathbf{x},\tilde{\mathbf{z}})$ is set to be the known values of $W(\tilde{\mathbf{z}}-\tilde{\mathbf{y}})$ calculated by the Random Walk algorithm as explained above.

Note that the points $\tilde{\mathbf{z}}$ can be sampled uniformly on the circles, then, instead of (2.20), the representation has the form

$$\mathbf{u}(\mathbf{x}) = E_\pi \left[\left\{ \Gamma(\mathbf{x}-\tilde{\mathbf{y}}) + \langle\, 2\pi\, p(\tilde{\mathbf{z}};\mathbf{x}) B(\mathbf{x},\tilde{\mathbf{z}})\,V(\tilde{\mathbf{z}},\tilde{\mathbf{y}}) \,|\, \tilde{\mathbf{y}} \,\rangle_{\tilde{\mathbf{z}}\in S(O_i,R_i)} \right\} \frac{\mathbf{f}(\tilde{\mathbf{y}})}{\pi(\tilde{\mathbf{y}})} \right] . \tag{2.21}$$

It is clear that for calculations, (2.20) is more attractive, since the singularity of the integral equation is here included into the density $p(\mathbf{z};\mathbf{x})$; in addition, the simulation algorithm according to this density is very simple and efficient (see [19]). However in some cases, it is desirable to use a distribution which is the same for all points $\mathbf{x}$, like the uniform distribution in (2.21).

Thus, let us describe a direct randomized calculation of the expectations in (2.20), which gives an approximate value of $\mathbf{u}(\mathbf{x})$ at a fixed point $\mathbf{x}$.

A direct randomized evaluation of the expectations in (2.20) can be designed in a form of a simple and efficient algorithm which we call here *Direct algorithm*. To present it in a detailed scheme, we first write down a *Direct unbiased estimator*:

$$\xi(\mathbf{x},\tilde{\mathbf{y}},\tilde{\mathbf{z}}) = \left[\Gamma(\mathbf{x}-\tilde{\mathbf{y}}) + B(\mathbf{x},\tilde{\mathbf{z}})V(\tilde{\mathbf{z}},\tilde{\mathbf{y}}) \right] \frac{\mathbf{f}(\tilde{\mathbf{y}})}{\pi(\tilde{\mathbf{y}})} \tag{2.22}$$

where

$$V(\tilde{\mathbf{z}},\tilde{\mathbf{y}}) = \begin{cases} -\Gamma(\tilde{\mathbf{z}}-\tilde{\mathbf{y}}) & if \quad \in \Gamma_i, \\ W(\tilde{\mathbf{z}},\tilde{\mathbf{y}}), & if \quad \in \gamma_i \qquad (i = 1,2)\ . \end{cases} \tag{2.23}$$

So if we now assume that $W(\tilde{\mathbf{z}},\tilde{\mathbf{y}})$ is known on γ_1 and γ_2, then in view of (2.20) we conclude that the estimator (2.22) is unbiased:

$$\mathbf{u}(\mathbf{x}) = E_{\tilde{\mathbf{y}},\tilde{\mathbf{z}}}\, \xi(\mathbf{x},\tilde{\mathbf{y}},\tilde{\mathbf{z}})\ .$$

The entries of $W(\tilde{\mathbf{z}},\tilde{\mathbf{y}})$ solve the problem (2.16), hence they can be precalculated on γ as mentioned above, by solving the linear algebraic equation (2.11) which approximates the integral equation (2.8). To solve

(2.11), one of the following methods can be used: (1) SOR method, (2) direct inversion of the matrix A, (3) a SOR based Random Walk as described in [20]. We note that (1) and (2) give the solution at the grid points on $\gamma = \gamma_1 \cup \gamma_2$ while the method (3) gives the solution at an arbitrary fixed point on γ. Clearly, all these three methods produce a bias in the estimator ξ. This bias can be made smaller by increasing the number of nodes on γ in the methods (1) and (2), or by increasing the number of Random Walks in the method 3.

Thus assuming that $W(\tilde{\mathbf{z}}, \tilde{\mathbf{y}})$ is calculated by one of these three methods described in [20], we present the *Direct algorithm* as follows:

Direct algorithm.

0. Put the initial score as zero: $\Xi(\mathbf{x}) = 0$.

1. Sample a random point $\tilde{\mathbf{y}}$ in our domain D according to a density $\pi(\mathbf{y})$ (say, uniformly in D), and suppose the sampled point lies in the disc $K(O_i, R_i)$ $(i = 1, 2)$.

2. On the circle $S(O_i, R_i)$ one samples a random point $\tilde{\mathbf{z}}$ according to the density $p_{R_i}(\mathbf{z}; \mathbf{x})$.

3. If the sampled point $\tilde{\mathbf{z}}$ belongs to the external boundary, i.e., if $\tilde{\mathbf{z}} \in \Gamma_i$, then calculate

$$\xi(\mathbf{x}, \tilde{\mathbf{y}}, \tilde{\mathbf{z}}) = \Big[\Gamma(\mathbf{x} - \tilde{\mathbf{y}}) - B(\mathbf{x}, \tilde{\mathbf{z}}) \Gamma(\tilde{\mathbf{z}} - \tilde{\mathbf{y}}) \Big] \frac{\mathbf{f}(\tilde{\mathbf{y}})}{\pi(\tilde{\mathbf{y}})} \, . \tag{2.24}$$

If $\tilde{\mathbf{z}} \in \gamma$, then $\Gamma(\tilde{\mathbf{z}} - \tilde{\mathbf{y}})$ should be replaced in (2.24) with $-W(\tilde{\mathbf{z}}, \tilde{\mathbf{y}})$ precalculated as described above. Note that when applying for this purpose the Random Walk method, we can replace $W(\tilde{\mathbf{z}}, \tilde{\mathbf{y}})$ by the relevant random estimator along one path of the Random Walk.

4. $\Xi(\mathbf{x}) := \Xi(\mathbf{x}) + \xi(\mathbf{x}, \tilde{\mathbf{y}}, \tilde{\mathbf{z}})/N$.

5. Repeating the steps 1-4 N times, N sufficiently large, we get the approximate solution as $\mathbf{u}(\mathbf{x}) \approx \Xi(\mathbf{x})$.

Note that in this algorithm we actually have to resolve the homogeneous boundary value problem (2.16) for N different boundary functions $-\Gamma(\mathbf{z} - \tilde{\mathbf{y}}_j)$, $j = 1, \ldots, N$. Hence if N is large, it may be time consuming. But to achieve high accuracy, N should be large enough.

To improve the efficiency, we use the symmetry property of the Green tensor $G(\mathbf{x}, \mathbf{y})$ in accordance with the so-called global Monte Carlo algorithm given in [16]. The symmetry property $G(\mathbf{x}, \mathbf{y}) = G^T(\mathbf{y}, \mathbf{x})$ implies that the evaluation of $W^{(i)}(\mathbf{x}, \mathbf{y})$, $i = 1, 2$ at the point $\mathbf{x}$ considered as the solution of the boundary value problem (2.16) with boundary function $-\Gamma^{(i)}(\cdot, \mathbf{y})$ ($i = 1, 2$, $\mathbf{y}$ fixed) is equivalent to evaluation of $W^{(i)}(\mathbf{x}, \mathbf{y})$, $i = 1, 2$ in point $\mathbf{y}$ with the boundary function $-\Gamma^{(i)}(\mathbf{x}, \cdot)$ ($i = 1, 2$, $\mathbf{x}$ fixed).

In this method, when calculating the Green function $G(\mathbf{x}, \mathbf{y})$ in many points $\tilde{\mathbf{y}}_j$, $j = 1, \ldots, N$ we have to solve only one boundary value problem with the boundary function $-\Gamma^{(i)}(\mathbf{x}, \cdot)$ ($i = 1, 2$, $\mathbf{x}$ fixed) but the solution is to be calculated in many points $\tilde{\mathbf{y}}_j$, $j = 1, \ldots, N$.

Formally written this means, we have to get the solution in $\tilde{\mathbf{y}}_j$, $j = 1, \ldots, N$ of the following two ($i = 1, 2$) boundary value problems (differential operators do here act on the variable $\mathbf{y}$, while $\mathbf{x}$ is fixed)

$$\Delta_{\mathbf{y}} \mathbf{W}^{(i)}(\mathbf{y}, \mathbf{x}) + \alpha \operatorname{grad} \operatorname{div} \mathbf{W}^{(i)}(\mathbf{y}, \mathbf{x}) = 0, \quad \mathbf{x} \in D, \quad \mathbf{W}^{(i)}(\mathbf{y}, \mathbf{x})|_{\mathbf{y} \to \mathbf{z} \in \partial D} = -\Gamma^{(i)}(\mathbf{z}, \mathbf{x}) \, . \tag{2.25}$$

Hence, we can write down an unbiased *adjoint estimator.*

Adjoint estimator

$$\eta(\mathbf{x},\tilde{\mathbf{y}},\tilde{\mathbf{z}}) = \Big[\Gamma(\mathbf{x}-\tilde{\mathbf{y}}) + B(\mathbf{y},\tilde{\mathbf{z}})V(\tilde{\mathbf{z}},\mathbf{x})\Big]\frac{\mathbf{f}(\tilde{\mathbf{y}})}{\pi(\tilde{\mathbf{y}})} \tag{2.26}$$

where

$$V(\tilde{\mathbf{z}},\mathbf{x}) = \begin{cases} -\Gamma(\tilde{\mathbf{z}}-\mathbf{x}) & if \quad \in \Gamma_i, \\ W(\tilde{\mathbf{z}},\mathbf{x}), & if \quad \in \gamma_i \qquad (i=1,2)\ . \end{cases} \tag{2.27}$$

From this we arrive at the adjoint algorithm.

Adjoint algorithm.

0. Put the initial score as zero: $\Xi^*(\mathbf{x}) = 0$.

1. The same as in the *Direct algorithm*, sample a random point $\tilde{\mathbf{y}}$ in our domain D according to a density $\pi(\mathbf{y})$ and suppose the sampled point lies in the disc $K(O_i,R_i)$ $(i=1,2)$.

2. For this value of $\tilde{\mathbf{y}}$, one samples on the circle $S(O_i,R_i)$ a random point $\tilde{\mathbf{z}}$ according to the density $p_{R_i}(\mathbf{z};\tilde{\mathbf{y}})$.

3. If the sampled point $\tilde{\mathbf{z}}$ belongs to the external boundary, i.e., if $\tilde{\mathbf{z}} \in \Gamma_i$, then calculate

$$\eta(\mathbf{x},\tilde{\mathbf{y}},\tilde{\mathbf{z}}) = \Big[\Gamma(\mathbf{x}-\tilde{\mathbf{y}}) - B(\tilde{\mathbf{y}},\tilde{\mathbf{z}})\Gamma(\tilde{\mathbf{z}}-\mathbf{x})\Big]\frac{\mathbf{f}(\tilde{\mathbf{y}})}{\pi(\tilde{\mathbf{y}})}\ . \tag{2.28}$$

If $\tilde{\mathbf{z}} \in \gamma_i$, then $\Gamma(\tilde{\mathbf{z}}-\mathbf{x})$ should be replaced in (2.28) with $-W(\tilde{\mathbf{z}},\mathbf{x})$ precalculated as described above. Here too, when applying for this purpose the Random Walk method, we can replace $W(\tilde{\mathbf{z}},\mathbf{x})$ by the relevant random estimator along one path of the Random Walk.

4. $\Xi^*(\mathbf{x}) := \Xi^*(\mathbf{x}) + \eta(\mathbf{x},\tilde{\mathbf{y}},\tilde{\mathbf{z}})/N$.

5. Repeating the steps 1-4 N times, N sufficiently large, we get the approximate solution as $\mathbf{u}(\mathbf{x}) \approx \Xi^*(\mathbf{x})$.

The main difference between the direct and adjoint algorithms can be explained as follows. In the direct algorithm, the solution at a point $\mathbf{x}$ is obtained as an average over N solutions of N boundary value problems with N random boundary functions $\Gamma(\tilde{\mathbf{z}}-\tilde{\mathbf{y}})$ generated by N random points $\tilde{\mathbf{y}}$ sampled in D, evaluated at the fixed point $\mathbf{x}$. In the adjoint algorithm, a solution of only one boundary value problem with boundary function $\Gamma(\tilde{\mathbf{z}}-\mathbf{x})$ is calculated, but for N random points $\tilde{\mathbf{y}}$ sampled in D with the density $\pi(\mathbf{y})$, and then one takes the spatial average over these N points.

Note that if we consider the Green tensor $G(\mathbf{x},\mathbf{y}) = \Gamma(\mathbf{x},\mathbf{y}) + W(\mathbf{x},\mathbf{y})$ (as well as the direct estimator $\xi(\mathbf{x},\tilde{\mathbf{y}},\cdot)$) as a random field generated by the random boundary function $-\Gamma(\mathbf{z}-\mathbf{y})$ (in turn, generated by the distribution $\pi(\mathbf{y})$) then this field obeys an ergodic property in the sense that the average of $G(\mathbf{x},\mathbf{y})f(\mathbf{y})/\pi(\mathbf{y})$ over the ensemble of boundary functions $\Gamma(\tilde{\mathbf{z}}-\tilde{\mathbf{y}})$ evaluated at a fixed point $\mathbf{x}$ equals the average of $G(\mathbf{y},\mathbf{x})f(\mathbf{y})/\pi(\mathbf{y})$ taken over spatial points $\mathbf{y}$ distributed in D with the density $\pi(\mathbf{y})$.

Remark. *The Adjoint algorithm is obviously efficient if the number of points* $\mathbf{x}$ *where the solution is calculated is not large, say, it is desired to calculate the solution in several fixed points. This is the case, when one calculates correlation functions along a chosen direction, for instance as in our case, the longitudinal and transverse correlation functions.*

The Direct algorithm is more efficient if the number of points where the solution is constructed is large while the volume forces $\mathbf{f}$ *are concentrated in a small subregion of D, or they are presented as a set of*

point sources.

This is a general heuristic comparative characteristics of the two methods. To compare their efficiencies, one needs also to compare the costs of calculations of the direct and adjoint estimators, and their variances. Indeed, assume the variance of the adjoint estimator (2.26) is much larger than that of (2.22) due to larger dispersion of the solution in the domain compared to the variance of the boundary functions. This may discard the advantages of the adjoint method.

3. Random load fields

The random loads $\mathbf{f}(\mathbf{x})$ are considered as an isotropic vector gaussian random field with a given spectral tensor $S_{ij}(\mathbf{k})$ defined as a Fourier transform of the correlation tensor $B_{ij}(\mathbf{r})$

$$S_{ij}(\mathbf{k}) = \frac{1}{(2\pi)^2} \int\limits_{R^2} B_{ij}(\mathbf{r}) e^{-i(\mathbf{r}\cdot\mathbf{k})} d\mathbf{r}, \quad i = 1,2 \ , \tag{3.1}$$

hence

$$B_{ij}(\mathbf{r}) = < f_i(\mathbf{x}) f_j(\mathbf{x}+\mathbf{r}) > = \int\limits_{R^2} S_{ij}(\mathbf{k}) e^{i(\mathbf{r}\cdot\mathbf{k})} d\mathbf{k} \ . \tag{3.2}$$

The spectral tensor of the isotropic random field $\mathbf{f}(\mathbf{x})$ has the following general structure [10]:

$$S_{ij}(\mathbf{k}) = [S_{LL}(k) - S_{NN}(k)] \frac{k_i k_j}{k^2} + S_{NN}(k)\delta_{ij} \ , \qquad k = |\mathbf{k}| \ . \tag{3.3}$$

Here S_{LL} and S_{NN} are longitudinal and transversal spectra, respectively. We consider incompressible random field $\mathbf{f}(\mathbf{x})$, for which div $\mathbf{f}(\mathbf{x}) = 0$. In this case, $S_{LL}(k) = 0$ and $S_{ij}(\mathbf{k}) = S_{NN}(k)P(\mathbf{k})$, where $P(\mathbf{k}) = (\delta_{ij} - \frac{k_i k_j}{k^2})$ is a projection tensor with δ_{ij} defined as the usual Kronecker delta symbol. Then

$$S_{NN}(k) = E(k)/(2\pi k) \ , \tag{3.4}$$

where $E(k)$ is an energy spectrum. We choose

$$E(k) = \sigma^2 \frac{2\sqrt{L}}{\sqrt{\pi}} e^{-Lk^2}, \quad k = |\mathbf{k}| \ ,$$

here L is a positive parameter, characterizing the correlation length.

For modelling the random field $\mathbf{f}(\mathbf{x})$, the Randomization spectral method for gaussian fields with given energy spectrum $E(k)$ can be applied. We use the following simulation formulae for the incompressible random vector field [16]:

$$\mathbf{f}(\mathbf{x}) \approx \mathbf{f}_m(\mathbf{x}) = \frac{\sigma}{\sqrt{m}} \sum_{l=1}^{m} P(\mathbf{k}_l) \left[\xi_l \cos(\mathbf{k}_l \cdot \mathbf{x}) + \eta_l \sin(\mathbf{k}_l \cdot \mathbf{x}) \right] \ , \tag{3.5}$$

where $\sigma^2 = \int_0^\infty E(k)dk$, $\mathbf{k}_j = k_j \omega_j$, k_j are independent random wave numbers are sampled according to the density $p = E(k)/\sigma^2$, and ω_l, $l = 1,\ldots,m$ is a family of mutually independent random vectors distributed uniformly on the unit sphere in $2D$; ξ_l, η_l $l = 1,\ldots,m$, are standard gaussian random vectors mutually independent and independent of $\mathbf{k}_l$.

To test the code written according the simulation procedure (3.5) described above we calculated the correlation tensor B_{ij}. Since we deal with the isotropic case, the correlation tensor is defined uniquely by two scalar functions, namely B_{LL} and B_{NN}, the longitudinal and transverse correlation functions, respectively.

$$B_{ij}(\mathbf{r}) = [B_{LL}(r) - B_{NN}(r)]\,\frac{r_i r_j}{r^2} + B_{NN}(r)\delta_{ij}\ , \quad r = |\mathbf{r}|\ . \tag{3.6}$$

So it is enough to calculate the correlation tensor as a function of r_1, for $r_2 = 0$. Due to (3.6), along the axes r_1 the vectors f_1 and f_2 are uncorrelated, so we calculate the functions $B_{ii}(r_1) = \langle f_i(0) f_i(r_1)\rangle$, $i = 1,2$. These functions can be evaluated explicitly.

Indeed, from (3.2), (3.3), and (3.4) we obtain after some evaluations of standard integrals (e.g., see [5])

$$\begin{aligned} B_{ij}(r_1) &= \int\limits_{\mathbf{R}}\int\limits_{\mathbf{R}} S_{ij}(\mathbf{k})\, e^{i(\mathbf{r}\cdot\mathbf{k})} d\mathbf{k} \\ &= \frac{\sigma^2\sqrt{L}}{\pi\sqrt{\pi}} \int\limits_0^\infty e^{-Lk^2}\, dk \int\limits_0^{2\pi} e^{ikr_1\cos(\varphi)} \begin{pmatrix} \sin^2(\varphi) & -\cos(\varphi)\sin(\varphi) \\ -\cos(\varphi)\sin(\varphi) & \cos^2(\varphi) \end{pmatrix} d\varphi \\ &= \frac{\sigma^2}{2} e^{-r_1^2/8L} \begin{pmatrix} I_0(r_1^2/8L) + I_1(r_1^2/8L) & 0 \\ 0 & I_0(r_1^2/8L) - I_1(r_1^2/8L) \end{pmatrix} \end{aligned} \tag{3.7}$$

where I_0, I_1 are the modified Bessel functions of the first kind.

Note that (3.7) does not imply that the correlation tensor B_{ij} is diagonal; it is diagonal only along the chosen direction $x = r_1$. From (3.6) and (3.7), $B_{11} = B_{LL}$, $B_{22} = B_{NN}$, so we will also call B_{11} and B_{22} longitudinal and transverse correlation functions, respectively. Note that $B_{LL}(0) = B_{NN}(0) = \langle|\mathbf{f}|^2\rangle/2$ in accordance with the theory of isotropic random fields [23].

4. Random Walk methods and Double Randomization

Assume we have to solve a PDE which includes a random field σ, say in the right-hand side, in coefficients, or in the boundary conditions:

$$Lu(\mathbf{x},\sigma) = f(\mathbf{x},\sigma), \quad u|_\Gamma = u_\gamma\ .$$

To solve this problem directly by constructing the ensemble of solutions via conventional numerical methods like finite elements or finite difference schemes is a hard task, which is not realistic for most practical problems. If however one of the Random Walk Methods can be applied, then a technique we call a Double Randomization Method is very useful. Let us describe it shortly.

Suppose we have constructed a stochastic method for solving this problem, for a fixed sample of σ. This implies, e.g., that an unbiased random estimator $\xi(\mathbf{x}|\,\sigma)$ is defined so that for a fixed σ,

$$u(\mathbf{x},\sigma) = \langle\xi(\mathbf{x}|\,\sigma)\rangle$$

where $\langle\cdot\rangle$ stands for averaging over the random trajectories of the stochastic method (e.g., a diffusion process, a Random Walk on Spheres, or a Random Walk on Boundary, e.g., see [16]).

Let us denote by E_σ the average over the distribution of σ.

The double randomization method is based on the equality:

$$E_\sigma u(\mathbf{x},\sigma) = E_\sigma \langle \xi(\mathbf{x}|\,\sigma)\rangle \ .$$

The algorithm for evaluation of $E_\sigma u(\mathbf{x},\sigma)$ then reads:

1. Choose a sample of the random field σ.

2. Construct a sample of the random walk along which the random estimator $\xi(\mathbf{x}|\,\sigma)$ is calculated.

3. Repeat 1. and 2. N times, and take the arithmetic mean.

Suppose one needs to evaluate the covariance of the solution. Let us denote the random trajectory by ω. It is not difficult to show [16] that

$$\langle u(\mathbf{x},\sigma)\,u(\mathbf{y},\sigma)\rangle = E_{(\omega_1,\omega_2,\sigma)}[\xi_{\omega_1}(\mathbf{x}|\sigma)\xi_{\omega_2}(\mathbf{y}|\sigma)] \ .$$

The algorithm for calculation of $\langle u(\mathbf{x},\sigma)\,u(\mathbf{y},\sigma)\rangle$ follows from this relation:

1. Choose a sample of the random field σ.

2. Having fixed this sample, construct two conditionally independent trajectories ω_1 and ω_2, starting at $\mathbf{x}$ and $\mathbf{y}$, respectively, and evaluate $\xi_{\omega_1}(\mathbf{x}|\sigma)\xi_{\omega_2}(\mathbf{y}|\sigma)$

3. Repeat 1. and 2. N times, and take the arithmetic mean.

Remark. Note that for the correlation function we can derive a closed equation. Indeed, assume that we have a linear scalar PDE with random right-hand side and zero boundary values

$$Lu = f, \quad \mathbf{x}\in D, \quad u|_\Gamma = 0,$$

where the random field f (not necessarily homogeneous) has $B_f(\mathbf{x},\mathbf{y})$ as its correlation function.

The solution u can be represented through the Green formula

$$u(\mathbf{x}) = \int\limits_D G(\mathbf{x},\mathbf{y})f(\mathbf{y})d\mathbf{y}$$

where $G(\mathbf{x},\mathbf{y})$ is the Green function for the domain D.

Under certain smoothness conditions we can prove that the correlation function of the solution $B_u(\mathbf{x},\mathbf{y}) = \langle u(\mathbf{x})u(\mathbf{y})\rangle$ and the input correlation function $B_f(\mathbf{x},\mathbf{y}) = \langle f(\mathbf{x})f(\mathbf{y})\rangle$ are related by the iterated equation

$$L_\mathbf{x} L_\mathbf{y} B_u(\mathbf{x},\mathbf{y}) = B_f(\mathbf{x},\mathbf{y}) \tag{4.8}$$

with boundary conditions $B_u|_{\mathbf{y}\in\Gamma} = 0$, $L_\mathbf{y}B(\mathbf{x},\mathbf{y})|_{\mathbf{x}\in\Gamma} = 0$. Here $L_\mathbf{x}$ implies that the operator L acts with respect to the variable $\mathbf{x}$, for fixed $\mathbf{y}$.

This can be derived as follows. First, starting from the definition $B_u(\mathbf{x},\mathbf{y}) = \langle u(\mathbf{x})u(\mathbf{y})\rangle$ we use the above Green formula to evaluate this product for the points $\mathbf{x}$ and $\mathbf{y}$, and change the product of integrals by the double integrals over the domain D; then we take the expectation under the double integral sign. This leads us to the representation

$$B_u(\mathbf{x},\mathbf{y}) = \langle u(\mathbf{x})u(\mathbf{y})\rangle = \int_D \int_D G(\mathbf{x},\mathbf{y}')\, G(\mathbf{y},\mathbf{y}'')\, B_f(\mathbf{y}',\mathbf{y}'')\rangle\, d\mathbf{y}' d\mathbf{y}'' \,. \tag{4.9}$$

It now remains to notice that the same expression is obtained by applying the Green formula successively to the iterated equation (4.8).

These arguments work only in the case of scalar equations, e.g., in the case of Laplace operator $L = \Delta$, the boundary value problem (4.8) is

$$\Delta_{\mathbf{x}} \Delta_{\mathbf{y}} B_u(\mathbf{x},\mathbf{y}) = B_f(\mathbf{x},\mathbf{y})$$

with boundary conditions $B_u|_{\mathbf{y}\in\Gamma} = 0$, $\Delta_{\mathbf{y}} B(\mathbf{x},\mathbf{y})|_{\mathbf{x}\in\Gamma} = 0$.

For systems of PDEs the relevant expressions are more complicated. Let us consider our system of Lamé equations (2.12). In the notations used in (2.12)-(2.15) we consider the correlation tensor of the solution $B^{(u)}(\mathbf{x},\mathbf{y}) = \langle \mathbf{u}(\mathbf{x})\mathbf{u}^T(\mathbf{y})\rangle$, and the correlation tensor of the body forces $B^{(f)}(\mathbf{x},\mathbf{y}) = \langle \mathbf{f}(\mathbf{x})\mathbf{f}^T(\mathbf{y})\rangle$. Let $L = \Delta + \alpha\,\mathrm{grad}\,\mathrm{div}$ be the Lamé operator. In accordance with (2.25), the Lamé operator L acts on a matrix W column-wise. This means, the matrix equation $LW = B$ (B is a matrix) is a pair of Lamé equations written for the relevant first and second columns of matrices W and B.

Now we are in a position to present the generalization of (4.9) to the system of Lamé equations. Analogously to the derivation of (4.9), after direct evaluations we arrive at

$$B^{(u)}(\mathbf{x},\mathbf{y}) = \int_D \int_D G(\mathbf{x},\mathbf{y}')\, B^{(f)}(\mathbf{y}',\mathbf{y}'') G^T(\mathbf{y},\mathbf{y}'') d\mathbf{y}' d\mathbf{y}'' \,. \tag{4.10}$$

It is also possible to write down a differential relation between the input matrix $B^{(f)}(\mathbf{y}',\mathbf{y}'')$ and the correlation matrix of the solution $B^{(u)}(\mathbf{x},\mathbf{y})$. Indeed, introduce a tensor $V(\mathbf{x},\mathbf{y})$, and write the following system of coupled systems

$$\begin{aligned} L_x B^{(u)}(\mathbf{x},\mathbf{y}) &= V^T(\mathbf{x},\mathbf{y}), \qquad B^{(u)}(\mathbf{x},\mathbf{y})|_{\mathbf{x}\in\Gamma} = 0, \\ L_y V(\mathbf{x},\mathbf{y}) &= [B^{(f)}(\mathbf{x},\mathbf{y})]^T, \qquad V(\mathbf{x},\mathbf{y})|_{\mathbf{y}\in\Gamma} = 0 \,. \end{aligned} \tag{4.11}$$

To prove that (4.10) solves the system (4.11), it is enough to notice that the representation (4.10) can be obtained by a successive application of the Green formula representation of the solutions to (4.11).

The system of equations (4.11) can be written as one system of 4-th order. Indeed, using the definition $\hat{L}V = LV^T$ we apply the operator $\hat{L}_y$ to both sides of the first equation in (4.11). This yields

$$\hat{L}_y L_x B^{(u)}(\mathbf{x},\mathbf{y}) = [B^{(f)}(\mathbf{x},\mathbf{y})]^T$$

with boundary conditions

$$B^{(u)}(\mathbf{x},\mathbf{y})|_{\mathbf{x}\in\Gamma} = 0, \qquad L_x B^{(u)}(\mathbf{x},\mathbf{y})|_{\mathbf{y}\in\Gamma} = 0 \,.$$

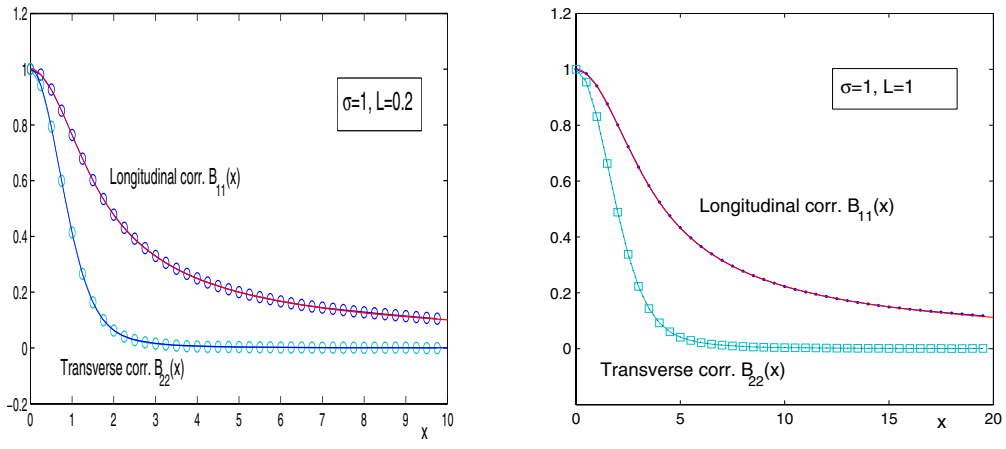

Figure 3: Transverse and longitudinal correlations: $L = 0.2$ (left panel), and $L = 1$ (right panel). In both cases, $\sigma = 1$, the number of harmonics $m = 100$, and $N = 10^5$ samples of random loads

5. Simulation Results

In this section we present the results of numerical experiments, and start with testing the used simulation procedure based on the Randomized spectral method.

5.1 Testing the simulation procedure for random loads

Now we can compare the results obtained by direct Monte Carlo calculations based on simulation formula (3.5) with the explicit functions (3.7). In Figure 3 we present the transverse and longitudinal correlations obtained by using 10^5 samples (circles) compared with the exact values evaluated by (3.7) (solid lines). It is seen that the accuracy is very high so that the calculated and exact results are practically coincident in these figures. Thus the simulation formula (3.5) with the chosen number of harmonics is accurate enough to use it in our numerical calculations.

5.2 Testing the Random Walk algorithm for non-zero body forces

To test the Random Walk algorithm described above in section 2.3 we solved the inhomogeneous problem (2.12) for two overlapped discs of unit radii, with the body force function with components

$$f_1(x_1,x_2) = 16(x_1^2+x_2^2-x_1) - 4 + \alpha(12x_1^2+4x_2^2-12x_1-2), \quad f_2(x_1,x_2) = 4\alpha x_2(2x_1-1)\ ,$$

the exact solution being $u_1 = (x_1^2+x_2^2)((x_1-1)^2+x_2^2-1), \quad u_2 = 0.$

In Figure 4 we compare the function u_1 obtained by the Random Walk algorithm against the exact results. The errors are less than 2.5%.

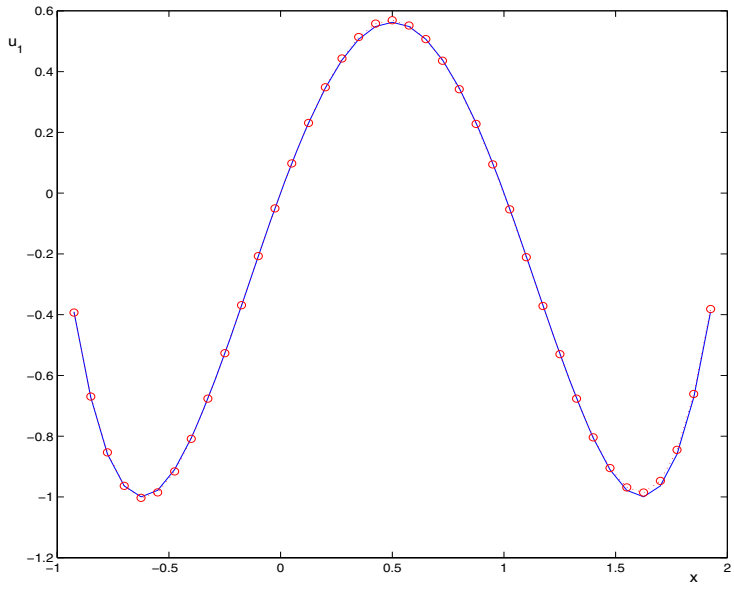

Figure 4: Comparison of an approximate solution obtained by the Random Walk algorithm (dots) with the exact result (solid line); $\alpha = 2$, the number of points sampled in the domain: $N = 100000$. Maximal error less than 2.5%.

5.3 Calculation of correlations for the displacement vector

The calculations were carried out for the two equal overlapped discs of radius $R = 1$; the first disc is centered at zero $(0,0)$, the second disc is centered at the point $(1,0)$. Thus the longitudinal coordinate $x = r_1$ varies from $x = -1$ to $x = 2$. In the numerical experiments we calculated the transverse and longitudinal correlations of the displacement vector between the point $x_0 = -0.5$ and the current point x varying between -0.5 and 1.9. The elastic constant μ was set to 1, so the calculations were made for different values of $\alpha = \lambda + 1$.

The random loads f_1 and f_2 (having zero mean values) were simulated by (3.5), with the intensity of fluctuations $\sigma = 1$, and different correlation length L. Note that $L = 1$ implies that the loads are strongly correlated since the radii of the discs are equal to 1, while $L = 0.001$ corresponds to an approximation of Gaussian white noise. The cases $L = 0.1 - 0.5$ are intermediate. In all calculations, we used the *Adjoint algorithm*.

In Figure 5 we present the transverse and longitudinal correlations for the displacement vector, normalized by the variance at the point $x_0 = -0.5$:

$$B_{11}^{(u)}(x) = \frac{\langle u_1(x_0)u_1(x)\rangle}{\langle u_1^2(x_0)\rangle} \tag{5.12}$$

for the longitudinal correlation, and

$$B_{22}^{(u)}(x) = \frac{\langle u_2(x_0)u_2(x)\rangle}{\langle u_2^2(x_0)\rangle} \tag{5.13}$$

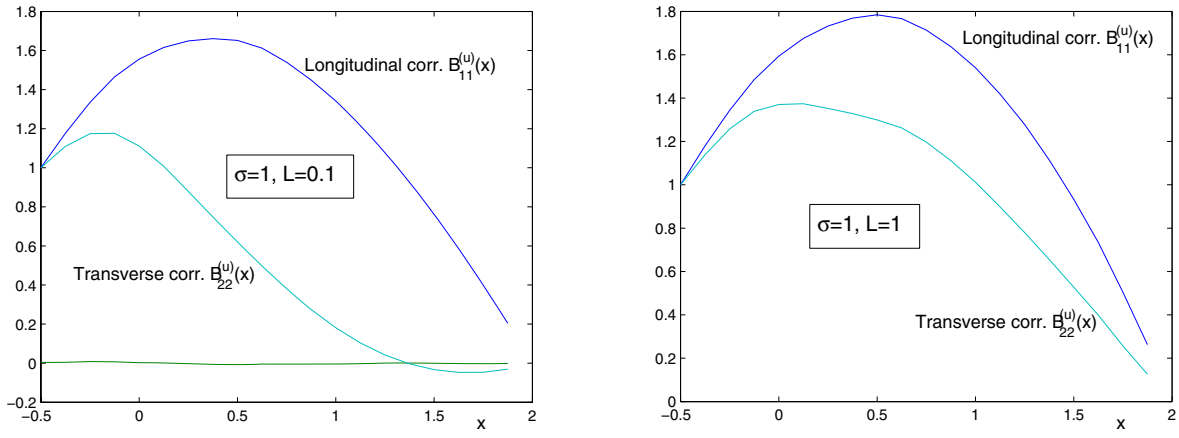

Figure 5: Transverse and longitudinal correlations: $L = 0.1$ (left panel), and $L = 1$ (right panel). In both cases, $\sigma = 1$, the number of harmonics $m = 100$, and $N = 10^5$ samples of random loads

for the transverse correlations.

It is seen from Figure 5 (right panel) that in the case when the correlation length is $L = 1$, the longitudinal correlation function has one maximum at a position about $x = 0.55$, and the transverse correlation function is positive. For $L = 0.1$ (left panel) this function becomes negative after $x = 1.4$, while the maximum of the longitudinal correlation function is attained at $x \approx 0.4$. Note that for larger value of L (equal to 0.5) the negative part disappears (see Figure 6, left panel), while for small values of L (equal to 0.001) the negative part begins already after $x = 0.2$ (right panel). It should be noted that in the latter case we have taken $\alpha = 10$ which also makes a considerable contribution to the increasing of the negative part of the transverse correlations. Indeed, for comparison, we present in Figure 7 the case of small correlation ($L = 0.001$) for $\alpha = 2$ (left panel) and $\alpha = 100$ (right panel) which clearly shows when compared to the figures in the right panel of Figure 6 that the larger the value of α, the larger the negative part of the transverse correlations.

Comparison of the direct Monte Carlo with a method based on the representation (4.10)

To test our method which we used to get the results presented in Figures (5)-(7) we compared it with the method based on the representation (4.10) and described above in section 4. In Figure 8, we compare the longitudinal and transverse correlations obtained by these two methods: the solid lines are the results obtained by the direct Monte Carlo algorithm, dots are the results obtained by the method of section 4. The difference between the results is less than 1% .

We also applied these two methods for calculation of the mean displacements under the same random loads f_1 and f_2 but having non-zero mean values: the curves of mean displacements presented in the left panel of Figure 9 correspond to the mean loads $\langle f_1 \rangle = 1$, $\langle f_2 \rangle = 1$, while the curves in the right panel were obtained for $\langle f_1 \rangle = 1$, $\langle f_2 \rangle = 0$. Note that in the latter case, the mean value of the second component is zero along the axis x_1. The results are in a good agreement, and the relatively large difference in the

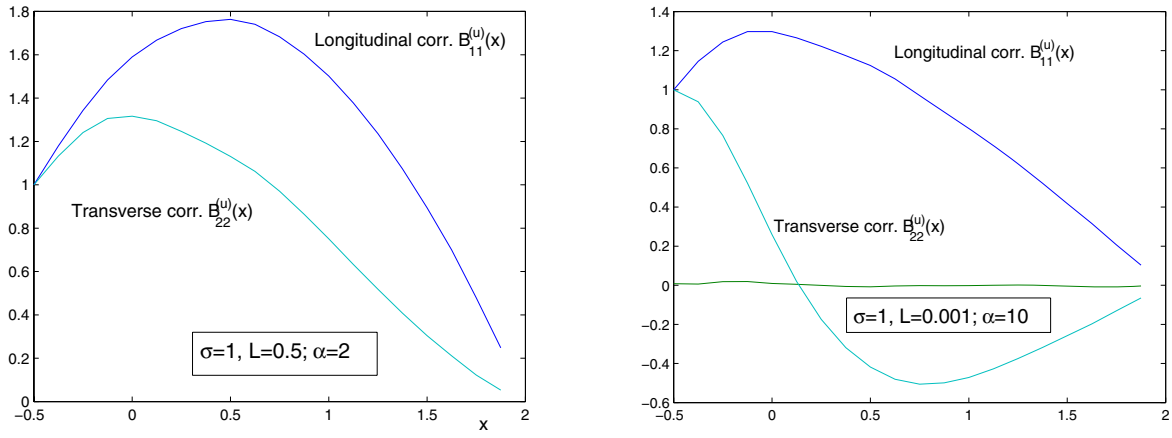

Figure 6: Transverse and longitudinal correlations: $L = 0.5$ (left panel), and $L = 0.001$ (right panel). In both cases, $\sigma = 1$, the number of harmonics $m = 100$, and $N = 10^5$ samples of random loads

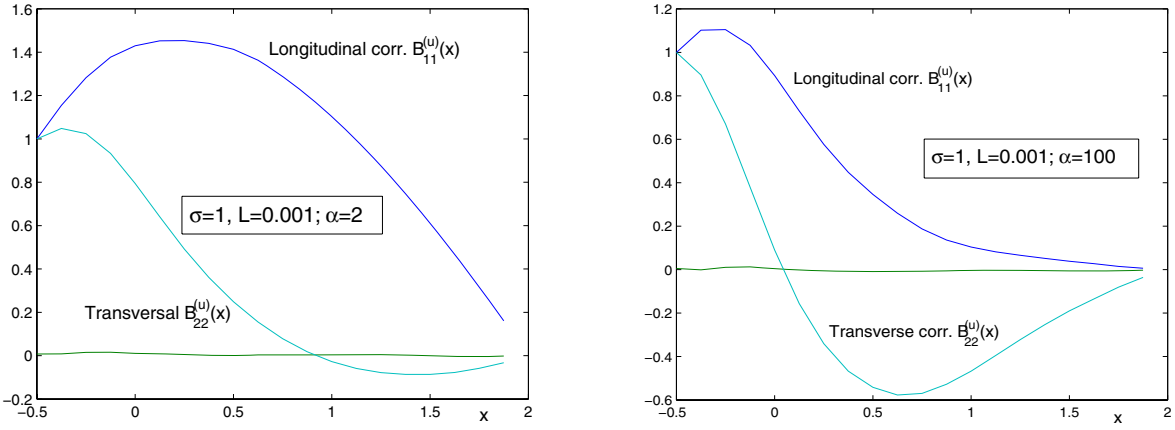

Figure 7: The same as in Figure 6, but for $L = 0.001$ (left panel), and $\alpha = 100$ (right panel).

transverse curves (right panel) can be decreased by increasing the number of trials.

The presented correlation functions can be informative enough to solve an inverse problem of finding the elastic constant α assuming the relevant correlations are known. In Figure 10 we show the longitudinal and transverse correlation functions for two values of α: $\alpha = 1$ and $\alpha = 2$ (left panel), and $\alpha = 10$ and $\alpha = 11$ (right panel). It seen from the curves of the left panel, that the longitudinal correlation function as almost unchanged, while the transverse correlation function is informative enough to see a clear difference between the cases $\alpha = 1$ and $\alpha = 2$. For larger values of α the longitudinal correlation function is more informative (see the right panel) but the difference between $\alpha = 10$ and $\alpha = 11$ is smaller. Note that this sensitivity analysis is made for the case of "white noise", i.e., when $L = 0.001$. We have repeated these calculations changing the value of L as $L = 1$, see the results in Figure 11. It is seen that this leads to more expressed difference of curves for different values of α with the exception that the longitudinal correlation functions for $\alpha = 10$ and $\alpha = 11$ almost coincide.

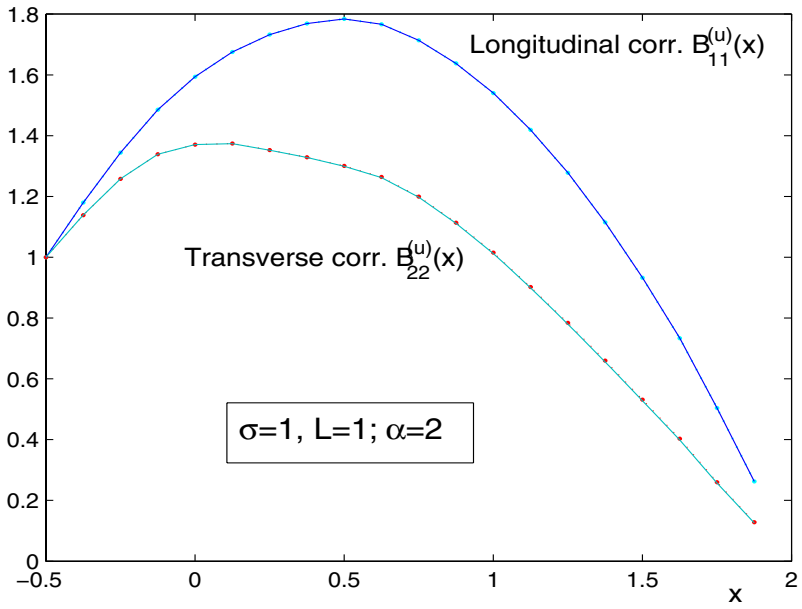

Figure 8: Comparison of direct Monte Carlo calculations (solid lines) with the results obtained by a numerical solution of the equation governing the correlation functions (dots) . The errors in calculations were everywhere less than 1%.

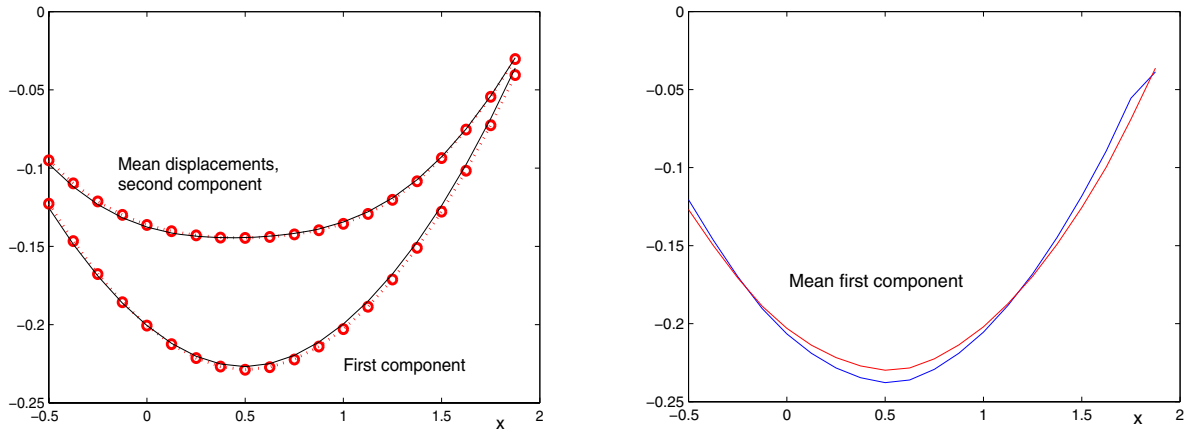

Figure 9: The vector of mean displacements. Left panel: dots - solution of the deterministic equation for the mean displacements under the mean loads $f_1 = 1$, $f_2 = 1$; solid lines - the mean displacements obtained by numerical simulation, for random loads with the same mean loads and gaussian fluctuations with $L = 1$, $\sigma = 1$. Right panel: the same as in left panel, but for the mean loads $f_1 = 1$, $f_2 = 0$; in this case the second component (u_2) is zero along the axis x_1 (not shown).

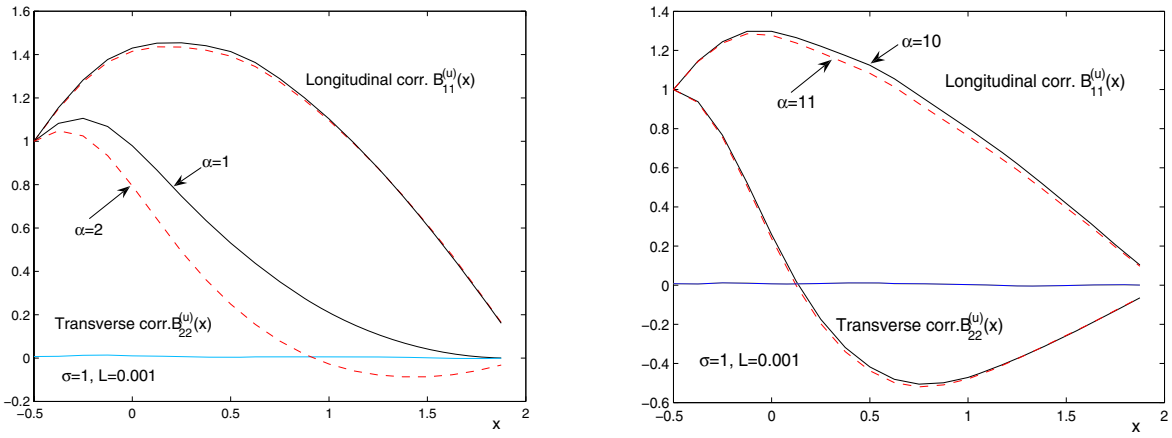

Figure 10: Sensitivity to the elasticity constant α: the correlation functions for $\alpha = 1$ (solid line) and $\alpha = 2$ (dots) are shown in left panel, and the case $\alpha = 10$ and $\alpha = 11$ is presented in the right panel.

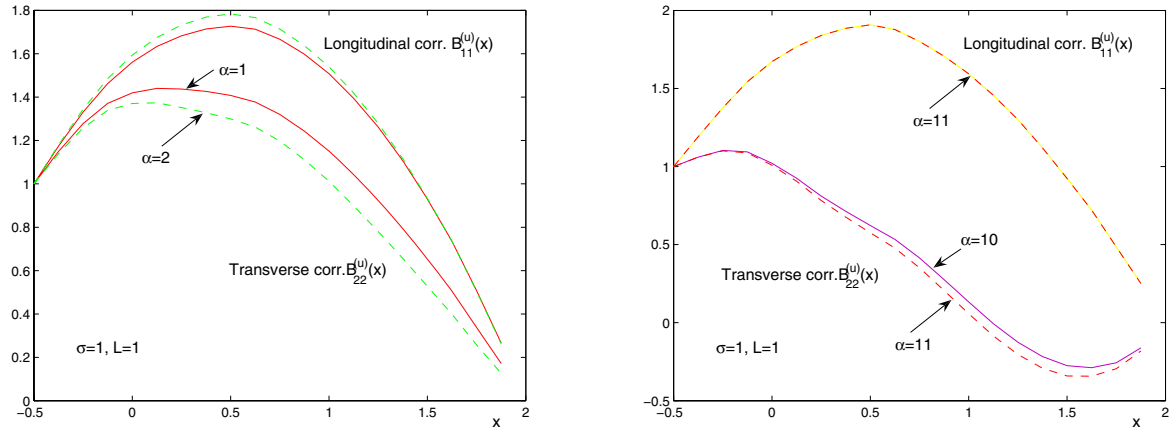

Figure 11: Sensitivity to the elasticity constant α: the same as in Figure 10, but for $L = 1$, the correlation functions for $\alpha = 1$ (solid line) and $\alpha = 2$ (dots) are shown in left panel, and the case $\alpha = 10$ and $\alpha = 11$ is presented in the right panel.

6. Conclusion and discussion

A stochastic simulation method for a numerical solution of the Lamé equation with random loads is suggested. To treat the general case of large intensity of random loads, we extend the Random Walk on Fixed Spheres (RWFS) method described in our paper [20] to non-zero body forces. The vector random field of loads is simulated by the Randomization Spectral method which takes explicitly into account the divergenceless and isotropy of the gaussian random loads. Comparative analysis of RWFS method and an alternative direct evaluation of the correlation tensor of the solution is made. We derive also a closed boundary value problem for the correlation tensor of the solution which is also applicable in the case of inhomogeneous random loads. Calculations of the longitudinal and transverse correlations are presented for a domain which is a union of two arbitrarily overlapped discs. Sensitivity calculation show that an inverse problem of determination of the elastic constants from the known longitudinal and transverse correlations of the loads can be solved by the suggested method. The algorithm and the calculations are given for a domain which is a union of two overlapping discs. However the method and the codes we have written are working for $2D$ domains consisting of a set of overlapping discs. It should be mentioned that for a special class of domains (the so-called DS_2 domains, see [20]) the method is especially efficient.

The method suggested can be generalized to (1) elasticity problems with other boundary conditions, (2) elasticity problems with random boundary functions, (3) problems with random elastic constants, (4) external boundary value problems. These problems are studied in our future paper.

References

[1] Maciej Anders, Muneo Hori. Stochastic finite element method for elasto-plastic body. International Journal for Numerical Methods in Engineering Volume 46 (1999), Issue 11, 1897 - 1916.

[2] G. Dagan. Flow and Transport in Porous Formations. Springer-Verlag, Berlin - Heidelberg, New York, 1989.

[3] R. Courant, D. Hilbert. *Methods of Mathematical Physics*, Volume 2, Wiley, 1989.

[4] Ermakov, S.M., Nekrutkin, W.W. and Sipin, A.S. *Random Processes for Classical Equations of Mathematical Physics.* vol. **34** of Math. Appl. (Soviet Series). Kluwer, Dodrecht, 1989.

[5] Gradstein, I.S. and Rygyk, I.M. *Tables of Integrals, Sums, Series and Products.* Nauka, Moscow, 1971 (in Russian).

[6] Kanevsky, V.A. and Lev, G.Sh. On simulation of the exit of a Wiener process from a ball. *Soviet J. on Numerical mathem. and mathem. physics* **17** (1977), No.3, 251-258.

[7] L.P. Khoroshun. Mathematical Models and Methods of the Mechanics of Stochastic Composites. International Applied Mechanics, 2000, Volume 36, Number 10, 1284-1316.

[8] Kurbanmuradov O. and Sabelfeld K.K. Stochastic spectral and Fourier-wavelet methods for vector Gaussian random field. Monte Carlo Methods and Applications, vol.12, N 5-6.

[9] C. Q. Li A stochastic model of severe thunderstorms for transmission line design. Probabilistic Engineering Mechanics, Vol. 15, 4, 359-364.

[10] A.S. Monin and A.M. Yaglom. *Statistical Fluid Mechanics: Mechanics of Turbulence*, Volume 2. The M.I.T. Press, 1981.

[11] Lawrence Nielsen, Robert F. Landel. Mechanical properties of polymers and composites. Second edition, Marcel Dekker, 1994.

[12] Niethanner W. The successive over relaxation method (SOR) and Markov chains. *Annals of Operations Research*, **103**, 351-358 (2001).

[13] J. Ophir, S. Alam, B. Garra et al. Elastography: Imaging the elastic properties of soft tissues with ultrasound. J. Med. Ultrasonics. 2002.

[14] S. Rahman, H. XU A Meshless Method for Computational Stochastic Mechanics. International Journal of Computational Engineering Science, 6:41-58, 2005.

[15] Sabelfeld, K.K. Vector Monte Carlo algorithms for solving systems of elliptic equations of the second order and the Lamé equation. *Dokl.Akad.Nauk SSSR*, **262** (1982), No.5, 1076–1080 (in Russian).

[16] Sabelfeld, K.K. *Monte Carlo Methods in Boundary Value Problems*. Springer-Verlag, Berlin – Heidelberg – New York, 1991.

[17] K. Sabelfeld. A method of random walks on fixed spheres for solving Neumann and mixed Neumann-Dirichlet boundary value problems. Proceedings of V IMACS Seminar on Monte Carlo methods. Tallahassee, USA, 2005, p.25-27.

[18] Sabelfeld, K.K. and Shalimova, I.A. *Spherical Means for PDEs.* VSP, The Netherlands, Utrecht, 1997.

[19] Sabelfeld, K.K. and Shalimova I.A. Random walk methods for static elasticity problems. *Monte Carlo Methods and Applications*, **8**, 2002, N2.

[20] K.K. Sabelfeld, I.A. Shalimova, and A.I. Levykin. Discrete random walk over large spherical grids generated by spherical means for PDEs. *Monte Carlo Methods and Applications*, **12** (2006), N 1.

[21] Sobolev, S.L. The Schwarz algorithm in elasticity theory. *Doklady AN SSSR*, **4** (1936), 235–238 (in Russian).

[22] Vanmarcke, E; Shinozuka, M; Nakagiri, S; Schueeller, G I; Grigoriu, M Random fields and stochastic finite elements. Structural Safety. Vol. 3, no. 3-4, pp. 143-166. 1986.

[23] A.M. Yaglom. Correlation theory of stationary and related random functions I. Basic results. Springer. New York, Heidelberg, Berlin, 1987.